

GENERALIZED PARTON DISTRIBUTIONS AT COMPASS

N. d'Hose¹

(1) *CEA-Saclay, DAPNIA-SPhN, F91191 Gif-sur-Yvette Cedex*
On behalf of the COMPASS collaboration

† *E-mail: ndhose@cea.fr*

Abstract

The Generalized Parton Distribution (GPD) framework is a novel and powerful tool for the investigation of the nucleon structure. Accessible through hard exclusive reactions the GPDs provide a three-dimensional picture of how the quarks and the gluons build up the nucleon. The high energies available at CERN, and the option of using either positive or negative polarized muon beams, make the fixed-target COMPASS set-up a unique place for studying GPDs, through Deeply virtual Compton scattering (DVCS). This contribution presents the goal of such experiments as well as the detectors necessary to complement the high resolution forward spectrometer COMPASS.

1 Quark and gluon imaging of the nucleon with GPDs

The GPD functions have been introduced 10 years ago [1, 2, 3] and they provide a comprehensive description of the quark and gluon structure of the nucleon (see Ref. [4, 5, 6] for reviews). GPDs describe the quantum-mechanical amplitude for "taking out" a parton (quark or gluon) of the wave function of the fast-moving nucleon and "putting it back" with a different momentum, giving a small momentum transfer to the nucleon (see Fig. 1).

Such a process can be probed by hard exclusive reactions such as Deeply Virtual Compton Scattering (DVCS) or meson production where a photon of virtuality Q^2 interacts with the active quark and where a real photon or a meson is ejected in order to compensate the energy flow in the hard scattering. The short-distance information specific to the process can be unambiguously separated from the long-distance information about nucleon structure contained in the GPDs (factorization theorem). The GPDs depend upon three kinematical variables: x , ξ and t . x is the average longitudinal¹ momentum fraction of the active quarks. $2\xi = 2x_{Bj}/(2 - x_{Bj})$ is the longitudinal momentum fraction of the transfer to the nucleon. $t = \Delta^2 = (\Delta_L + \Delta_T)^2$ is the squared transfer between

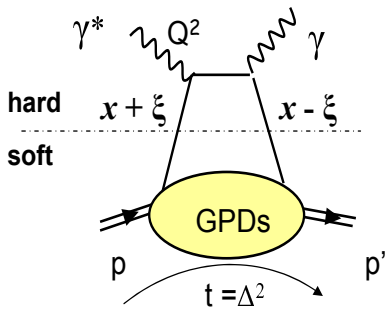


Figure 1. Handbag diagram for the DVCS amplitude at leading twist

the initial and final nucleons. The transverse transfer Δ_T leads to information about the spatial transverse distribution of partons.

¹"longitudinal" refers to the direction of the fast moving nucleon for example in the centre of mass of the virtual photon-nucleon collision

At leading twist four GPDs are necessary to parametrize the nucleon structure information. H and \tilde{H} are generalizations of the parton distributions measured in DIS. In the forward limit, corresponding to $\xi = 0$ and $t = 0$, H^q , for a quark of flavor q , reduces to the quark distribution $q(x)$ and \tilde{H}^q to the longitudinally polarized quark distribution $\Delta q(x)$ while for the gluon sector $H^g(x, 0, 0) = g(x)$ and $\tilde{H}^g(x, 0, 0) = \Delta g(x)$. H and \tilde{H} conserve the helicity of the proton, whereas E and \tilde{E} allow for the possibility of the proton helicity flip. In such a case the overall helicity is not conserved: the proton changes helicity but the massless quark does not, so that the angular momentum conservation implies a transfer of orbital angular momentum. This is only possible for nonzero transverse momentum transfer, which is new with respect to the ordinary parton distributions. The Ji sum rule relates the GPDs and the total angular momentum of the partons [2]:

$$\frac{1}{2} \sum_q \int_{-1}^{+1} dx x (H^q(x, \xi, t=0) + E^q(x, \xi, t=0)) = J^{quark} \quad (1)$$

The second moment at $t = 0$ gives the total (spin + orbital) angular momentum carried by the quarks. There is an equivalent sum rule for the gluons. The first moments of the GPDs are related to the nucleon elastic form factors. For example:

$$\sum_q e_q \int_{-1}^{+1} dx H^q(x, \xi, t) = F_1(t) \quad (2)$$

where F_1 is the Dirac form factor. However the GPDs contain much more information than the parton densities and the elastic form factors. They describe the correlation between a parton longitudinal momentum fraction, x , and the transverse momentum transfer to the nucleon, Δ_T . For $\xi = 0$, $H(x, 0, -\Delta_T^2)$ is the Fourier transform of the probability density to find a quark with momentum fraction x at a given distance b from the center of momentum in the transverse plane: $H(x, 0, -\Delta_T^2) = \int d^2b e^{-i\Delta_T \cdot b} f(x, b)$. This 1+2-dimensional "mixed" longitudinal momentum and transverse coordinate representation corresponds to a set of tomographic images of the parton distribution in the nucleon at a fixed longitudinal momentum fraction x (see Fig. 2).

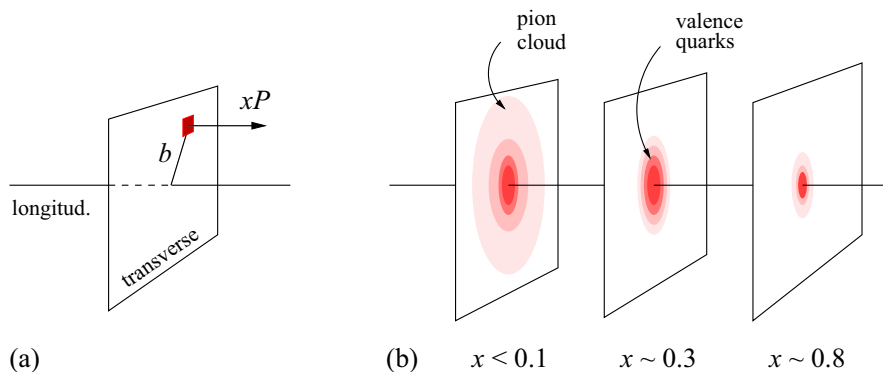


Figure 2. Nucleon tomography: (a) The transverse Fourier transform of the GPD describes the distribution of quarks with longitudinal momentum fraction x with respect to transverse position, (b) It produces a set of 1+2-dimensional "tomographic" image of the quark structure of the nucleon which allows to separate the contributions from the valence quarks or from the pion cloud or sea quarks. (The figures are from Refs [7, 8])

The width of the b distribution goes to zero as $x \rightarrow 1$ since the active quark becomes the center of momentum. At $x \sim 0.3$ one mainly "sees" the core of the valence quarks distributed over transverse distances $b \ll 1$ fm. At $x < 0.1$ the pion cloud becomes visible, extending over larger transverse distances $b \sim 1$ fm. At even smaller momentum fractions, $x < 0.01$ the observed partons are mostly the gluons and flavor singlet quarks produced by gluon radiation.

A large effort in the community since 10 years on both experimental and theoretical aspects has been undertaken and has provided more than 300 publications so far. Several models are emerging and the complex task of extracting information on the GPDs from the experimental observables is extensively discussed in the recent literature. Predictions made from lattice QCD [9, 10, 11] for the first moments of the nucleon GPDs confirm that the transverse size of the nucleon depends significantly on the momentum fraction x . In the chiral dynamics approach [12], the gluon density is generated by the "pion cloud" of the nucleon, and a significant increase in the overall transverse size of the nucleon is observed for x below the ratio of pion and proton masses m_π/m_p (see Fig. 3). The favored domain to see a transition in the transverse size is ranging from 10^{-2} to 10^{-1} , which is the kinematical COMPASS domain.

Experimental information about GPDs comes from hard exclusive processes, such as DVCS or meson production. The factorization [13] is valid when the finite momentum transfer $t = \Delta^2$ to the target remains small compared to the photon virtuality Q^2 . For meson production the factorization implies the extra condition that the virtual photon be longitudinally polarized. For DVCS, the experience with inclusive DIS and other two-photon processes suggests that the leading-twist approximation should be reliable at $Q^2 \sim 1$ GeV², which seems consistent with the first experimental results. For meson production, data on the pion form factor at high Q^2 suggest that higher-twist effects could give significant corrections to the GPD description up to Q^2 larger than a few GeV².

2 Role of COMPASS with the unique availability of high energy positive and negative muon beams

Thanks to the high energy of the muon beam available at COMPASS (between 100 and 190 GeV) the kinematical range covered by the proposed GPD programme experiment will be large enough to provide a bridge between the HERA collider experiments [14, 15, 16, 17] at very small x_{Bj} and the JLAB [18, 19, 20, 21] and HERMES [22, 23, 24] fixed target experiments at large x_{Bj} . Since the shutdown of HERA, the availability of positive and negative polarized muons at CERN gives to COMPASS the opportunity to measure the different configurations of charge and spin of the beam.

The experimental programme using COMPASS at CERN with a muon beam of 100

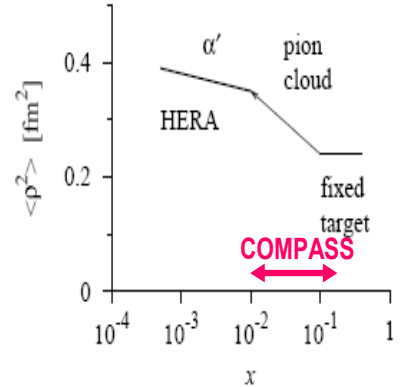


Figure 3. The average squared transverse radius of the gluon distribution in the nucleon (extracted from J/ψ photoproduction data) and the COMPASS kinematical domain.

GeV will give access to three bins in x_{Bj} (presented in Fig. 4):

$$x_{Bj} = 0.05 \pm 0.02 \quad x_{Bj} = 0.1 \pm 0.03 \quad x_{Bj} = 0.2 \pm 0.07$$

in a large range of Q^2 from 1 to 7 GeV² in order to control the Q^2 independence (scaling) predicted by the QCD factorization. Assuming 6 months of data taking and a muon flux of $2 \cdot 10^8 \mu$ per SPS spill, a reasonable statistics can be obtained for Q^2 values up to 7 GeV². It is worth noting that an increase of the number of muons per spill by a factor 2 would result in an increase in the range in Q^2 to about 11 GeV².

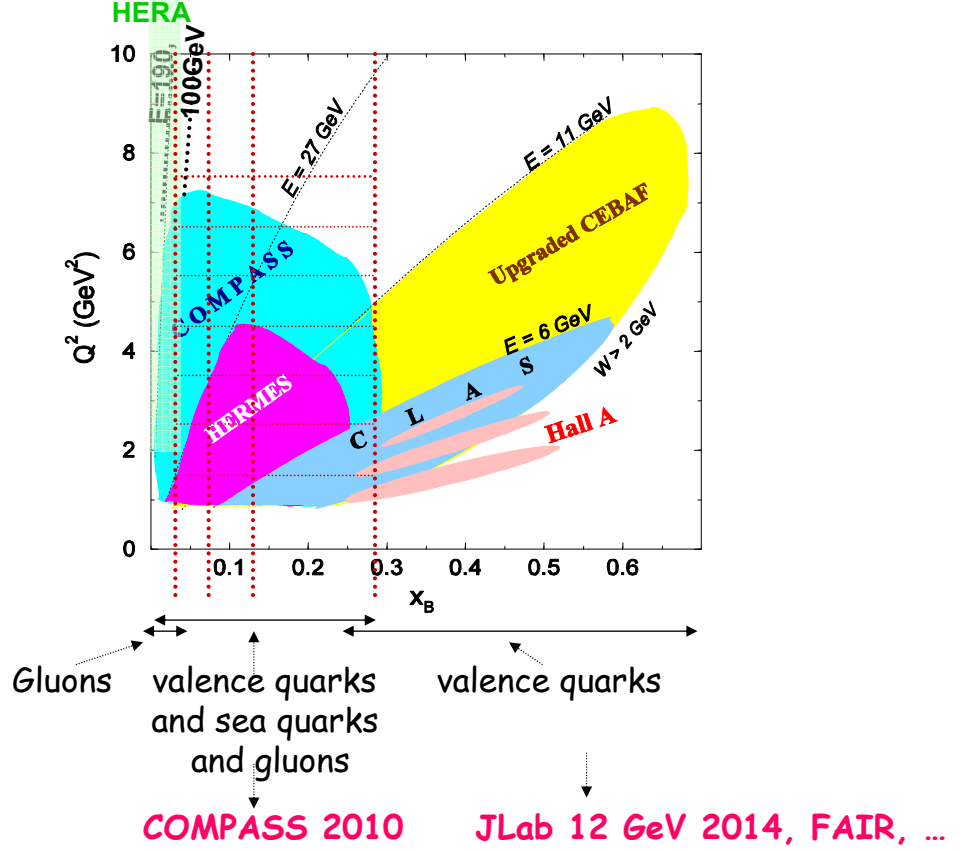


Figure 4. Kinematical coverage for all the experiments. Three bins in x_{Bj} can be investigated at COMPASS around 0.05, 0.1 and 0.2 and each one can be subdivided in sub-bins in Q^2 from 1 to 7 GeV².

3 The DVCS measurements at COMPASS

3.1 Experimental method

The DVCS amplitude at leading order has the form:

$$\mathcal{H} \sim \int_{-1}^{+1} \frac{H(x, \xi, t)}{x - \xi + i\epsilon} dx \sim \mathcal{P} \int_{-1}^{+1} \frac{H(x, \xi, t)}{x - \xi} dx - i\pi H(\xi, \xi, t) \quad (3)$$

where H stands for a generic GPD and \mathcal{P} for Cauchy's principal value integral.

Since GPDs are real valued due to time reversal invariance, the real and imaginary parts of the DVCS amplitude contain distinct information on GPDs. The imaginary part depends on the GPDs at the specific values $x = \xi$. The real part is a convolution of the GPDs with the kernel $1/(x-\xi)$ (see Eq. 3). To extract the GPDs from this convolution the strategy will be similar to the one used in DIS. The GPDs will be adequately parametrized and the parameters will be determined by a fit to the data. The real and imaginary parts can be accessed separately through the azimuthal dependence of the interference between DVCS and BH.

With muon beams one naturally reverses both charge and helicity at once. Practically μ^+ are selected with a polarization of -0.8 and μ^- with a polarization of +0.8. The precise method to extract these quantities with polarized positive and negative muon beams has been proposed by Diehl *et al.* [25, 26] and well established up to twist-3 contributions by Belitsky, Mueller and Kirchner [27]. Let us consider an unpolarized target and a muon beam of charge e_ℓ and longitudinal polarization P_ℓ . We can write:

$$\begin{aligned} \frac{d\sigma(\ell p \rightarrow \ell p \gamma)}{d\varphi} &= d\sigma^{BH} + d\sigma_{unpolarized}^{DVS} + P_\ell \times d\sigma_{polarized}^{DVS} \\ &+ e_\ell \times \mathcal{R}_e(Int_C) + e_\ell P_\ell \times \mathcal{I}_m(Int_S) \end{aligned} \quad (4)$$

Considering the sum or the difference of the cross section given by muons of opposite charge and polarization and using also the azimuthal angular dependence in φ the angle between the leptonic and hadronic planes, we can get the dominant twist-2 contributions of the Beam Charge and Single Spin Asymmetries for DVCS:

$$\begin{aligned} d\sigma(\mu^{+\downarrow}, \varphi) + d\sigma(\mu^{-\uparrow}, \varphi) &\propto \Im m(F_1 \mathcal{H} + \xi(F_1 + F_2) \tilde{\mathcal{H}} - t/4m^2 F_2 \mathcal{E}) \cdot \sin\varphi + \dots \\ d\sigma(\mu^{+\downarrow}, \varphi) - d\sigma(\mu^{-\uparrow}, \varphi) &\propto \Re e(F_1 \mathcal{H} + \xi(F_1 + F_2) \tilde{\mathcal{H}} - t/4m^2 F_2 \mathcal{E}) \cdot \cos\varphi + \dots \end{aligned} \quad (5)$$

F_1, F_2 are the Dirac, Pauli form factors, $\Re e \mathcal{H} = \mathcal{P} \int_{-1}^{+1} \frac{H(x, \xi, t)}{x-\xi} dx$, $\Im m \mathcal{H} = -i\pi H(\xi, \xi, t)$

Thanks to these last equations we can see that the small values of the kinematical factors ξ and t give a dominant contribution of the GPD H when using a proton target. In contrary with a neutron (or deuterium) target F_1 is negligible and this is a good case for a measurement of the GPD E contribution.

3.1.1 Projections for DVCS Beam Charge & Spin Asymmetry measurements

We propose to measure at COMPASS the quantities

$$\sigma(\mu^{+\downarrow}) - \sigma(\mu^{-\uparrow}), \sigma(\mu^{+\downarrow}) + \sigma(\mu^{-\uparrow}) \text{ and } \frac{\sigma(\mu^{+\downarrow}) - \sigma(\mu^{-\uparrow})}{\sigma(\mu^{+\downarrow}) + \sigma(\mu^{-\uparrow})} \quad (6)$$

This last ratio is called in the following, the Beam Charge & Spin Asymmetry (BC&SA).

Figure 5 shows the azimuthal distribution of the Beam Charge & Spin Asymmetry which could be measured at COMPASS using the 100 GeV muon beams for different (x_{Bj}, Q^2) domains. Statistical errors are evaluated for 150 days of data taking with a 25% global efficiency. The data allow for a good discrimination between different models. Predictions are made using the VGG model with different parametrizations.

The VGG model relies on the double distributions in x and ξ proposed by Radyushkin [3] to respect polynomiality conditions. Model 1 [28, 29] uses a simple ansatz to parametrize GPDs based on nucleon form factors and parton distributions and fulfills the GPD sum rules. Model 2 [28, 4, 29] is more realistic because it correlates the x and t dependence with a simple Regge-motivated ansatz. This takes into account the fact that the slow partons tend to stand at a larger distance from the nucleon centre than the fast partons. A gradual increase of the t -dependence of $H(x, 0, t)$ is seen as one goes from larger to smaller values of x . The parametrization: $H(x, 0, t) = q(x)e^{t \langle b_{\perp}^2 \rangle} = q(x)/x^{\alpha t}$ is used where $\langle b_{\perp}^2 \rangle = \alpha \cdot \ln 1/x$ represents the increase of the nucleon transverse size with energy. α is considered as a slope in Regge theory and is evaluated to 0.8 GeV^2 (Model 2) and 1.1 GeV^2 (Model 2*) (values which give rather good description of the proton Dirac form factor). α is related to the transverse size of partons inside the nucleon and a precise determination of the α parameter can be done at COMPASS. Other models including gluons contributions are under study.

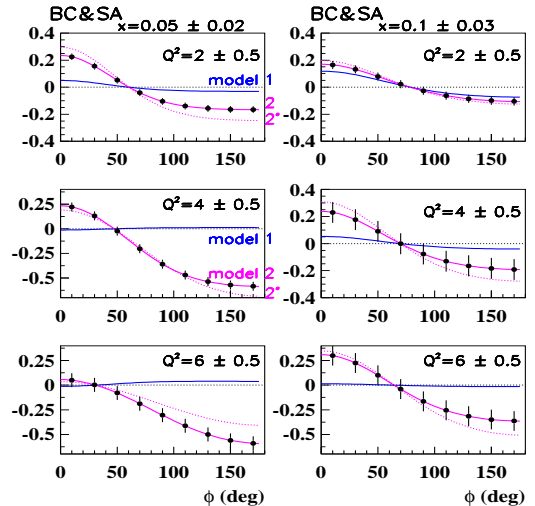


Figure 5. Projected error bars for a measurement of the azimuthal angular distribution of the BC&SA measurable at COMPASS at $E_{\mu} = 100 \text{ GeV}$ and $|t| \leq 0.6 \text{ GeV}^2$ for 2 domains of x_{Bj} (0.05 on left and 0.10 on right) and 3 domains of Q^2 (2,4,6 GeV^2) obtained in 150 days of data taking with a global efficiency of 25% and with $2 \cdot 10^8 \mu$ per SPS spill ($P_{\mu^+} = -0.8$ and $P_{\mu^-} = +0.8$) and a 2.5m long liquid hydrogen target. Predictions are made using the VGG model with different parametrizations (see the text)

4 The other measurements at COMPASS

4.1 The observables to get a spin/ flavor decomposition

The GPDs reflect the structure of the nucleon independently of the reaction which probes the nucleon. In this sense they are universal quantities and can be accessed, through DVCS or through the hard exclusive lepton production of mesons as $\pi^{0,\pm}, \eta, \dots, \rho^{0,\pm}, \omega, \phi, \dots$

The longitudinally polarized vector meson channels $\rho^{0,\pm}, \omega, \phi, \dots$ are sensitive at leading order only to the GPDs H and E while the pseudo-scalar channels $\pi^{0,\pm}, \eta, \dots$ are sensitive only to \tilde{H} and \tilde{E} [13]. In comparison we recall that DVCS depends on the four GPDs. This property makes the hard meson production reactions complementary to the DVCS process as it provides an additional tool or filter to disentangle the different GPDs.

Both quark and gluon GPDs contribute to the meson production at the same order in α_s . The decomposition on quark flavor and gluon contributions can be realized through the different combinations obtained with a set of mesons. For example:

$$H_{\rho^0} = \frac{1}{\sqrt{2}} \left(\frac{2}{3} H^u + \frac{1}{3} H^d + \frac{3}{8} H^g \right); \quad H_{\omega} = \frac{1}{\sqrt{2}} \left(\frac{2}{3} H^u - \frac{1}{3} H^d + \frac{1}{8} H^g \right); \quad H_{\phi} = -\frac{1}{3} H^s - \frac{1}{8} H^g$$

The complete experimental programme at COMPASS will comprise the measurement of DVCS cross section with polarized positive and negative muon beams and at the same time the measurement of a large set of mesons ($\rho, \phi, \omega, \pi, \eta, \dots$). This will provide different and complementary facets of the GPDs study.

4.2 The observables to get the GPD E

This GPD E is of high importance to determine the angular orbital momentum contribution to the nucleon spin puzzle. It enters in the Ji sum rule (1):

$$\frac{1}{2} \sum_q \int_{-1}^{+1} dx x (H^q(x, \xi, t=0) + E^q(x, \xi, t=0)) = J^{quark}$$

which is ξ -independent. Polarized DIS determines the forward limit of H^q . So:

$$M_q = \int_{-1}^{+1} dx x q(x) = \int_{-1}^{+1} dx x H^q(x, \xi=0, t=0)$$

meaning that the contribution of H^q to the Ji sum rule is known. Constraints on E^q come from the Pauli form factor

$$F_2(t) = \sum_q e_q \int_{-1}^{+1} dx E^q(x, \xi, t)$$

where e_q is the quark charge in units of the elementary charge [30, 31]. Further constraints on E^q will provide information related to the quark orbital momentum in the nucleon (see predictions in [4, 32]).

At leading order there are several promising ways to get the GPD E at COMPASS:

1. the Beam Charge and Single Spin Asymmetry for DVCS on the neutron (see Equ.(5));
2. the Transverse Target Spin Asymmetry for DVCS on the proton:

$$\begin{aligned} d\sigma(\varphi, \varphi_S) - d\sigma(\varphi, \varphi_S + \pi) &\propto \Im m(F_2 \mathcal{H} - F_1 \mathcal{E}) \cdot \sin(\varphi - \varphi_S) \cdot \cos\varphi \\ &+ \Im m(F_2 \tilde{\mathcal{H}} - F_1 \xi \tilde{\mathcal{E}}) \cdot \cos(\varphi - \varphi_S) \cdot \sin\varphi \end{aligned}$$

3. the Transverse Target Spin Asymmetry for vector meson (M) production induced by longitudinal virtual photon ² on the proton:

$$d\sigma(\varphi, \varphi_S) - d\sigma(\varphi, \varphi_S + \pi) \propto \Im m(\mathcal{E}_{\mathcal{M}}^* \mathcal{H}_{\mathcal{M}}) \cdot \sin(\varphi - \varphi_S)$$

where φ is the azimuthal angle between the lepton and hadron planes and φ_S the azimuthal angle of the target spin vector around the virtual photon direction.

Method 1 has been successfully investigated at JLab [21] on a deuterium target while the transverse asymmetries of methods 3 and 4 have been studied at HERMES both for DVCS and rho vector meson production [24].

Preliminary studies on the transverse target spin difference (see Fig.6) were already made with the present COMPASS set-up and the ⁶LiD polarized target [33]. Contributions from coherent scattering from the target nuclei and incoherent scattering from the quasi-free nucleons inside the target, have to be disentangled. Separation between longitudinal and transverse photon contributions is being performed thanks to the method proposed by Diehl *et al.* [34].

²for which factorization is valid

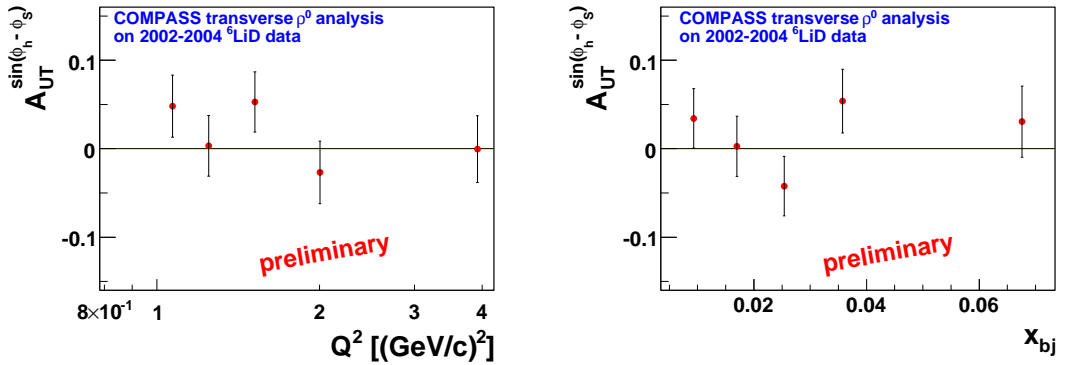


Figure 6. Transverse Target Spin Asymmetry obtained for the full 2002-3-4 sample with the ${}^6\text{LiD}$ target, which contains both, coherent contributions of the target nuclei and incoherent contributions of protons and neutrons. It contains also longitudinal and transverse virtual photon contributions.

5 General Request for the COMPASS apparatus

The goal of a GPD experiment is to measure absolute cross sections for the exclusive production of photons (DVCS) and a large set of mesons. This implies an accurate determination of the luminosity and acceptance and several tests will be done to achieve this objective.

The most demanding GPD measurement is the DVCS $\mu p \rightarrow \mu p \gamma$ which requires to select events with one (and only one) muon in the very forward direction, one (-id-) photon at moderate forward angle and one (-id-) slow recoiling nucleon. Many competing reactions can generate background:

- Deep π^0 production $\mu p \rightarrow \mu p \pi^0$ where the high energy γ from π^0 decay mimics the DVCS photon,
- Dissociation of the target $\mu p \rightarrow \mu(p\pi^0)\gamma$ where the extra π^0 is accompanying the slow proton,
- DIS with many outgoing particles such as π^0 which have to be identified.

The resolution in missing mass required to reject an extra pion is $(m_p + m_\pi)^2 - m_p^2 = 0.25 \text{ GeV}^2$. The experimental resolution which can be achieved at COMPASS energy is larger than 1 GeV^2 , therefore the missing mass energy selection using the energy balance of the scattered muon and photon is not accurate enough. The background from π^0 decay has to be removed directly by rejecting the associated low energy photon. The COMPASS spectrometer comprises two forward stages (see Fig. 7), one for angles up to 2° (after SM2) and one for angles up to 10° (after SM1). The photon detection has to be performed with excellent energy resolution and with high efficiency in a harsh environment of high flux and background. This puts strong constraints on the existing calorimetry and justifies the construction of a new calorimeter ECAL0 [35] to access larger angles of up to about 20° . In addition a 4m long recoil detector has to be built, surrounding the 2.5 m long H_2

(or D_2) target to measure precisely the type, number and momenta of charge particles, in order to ensure exclusivity of the selected reaction.

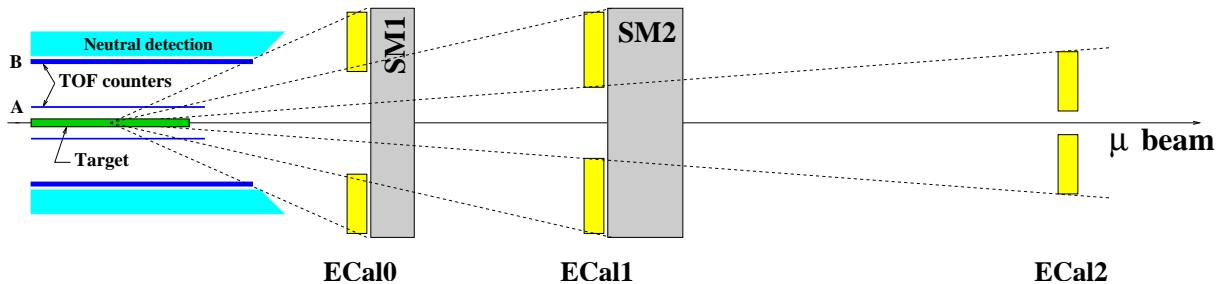


Figure 7. General principle of the COMPASS layout. At present COMPASS is a two stage spectrometer comprising many tracking and particle identification detectors grouped around the 2 dipole magnets SM1 and SM2. Only upgraded and new detectors (ECAL0, ECAL1, ECAL2, ToF, detector for neutral particles) discussed and specified in this report are shown.

6 Conclusion and Roadmap

For the GPD programme for 2010 and beyond, a 2.5 m long hydrogen target, a 4 m long recoil detector and a high-performance calorimetry are mandatory. Presently, a 40 cm long hydrogen target, and a 1 m long recoil detector are being designed for the hadron programme setup. The two existing calorimeters will be used to collect neutral particles such as π^0 and η in order to identify exotic mesons or glueballs. Since recoil proton detection and photon reconstruction are the two key experimental points of any DVCS experiment, the present hadron programme setup provides an excellent opportunity for a thorough preparation of the future DVCS setup. Although not optimized for a DVCS experiment, the available detectors can be used for preliminary studies and for quantitative evaluation of their performances. In addition, the versatility of the SPS M2 beam line makes it extremely easy to switch from a hadron beam to either positive or negative muon beam. Very preliminary tests will be requested during the 2008-9 COMPASS run. The goal is to demonstrate the feasibility of the DVCS experiments at COMPASS and to be ready for a complete GPD program after 2010 and before the outcome of other facilities as JLab 12 GeV around 2014. This gives an excellent opportunity for a unique program at COMPASS.

References

- [1] D. Mueller *et al.*, Fortsch. Phys. **42** (1994) 101.
- [2] X. Ji, Phys. Rev. Lett. **78** (1997) 610; Phys. Rev. **D 55** (1997) 7114.
- [3] A.V. Radyushkin, Phys. Lett. **B 385** (1996) 333; Phys. Rev. **D 56** (1997) 5524.
- [4] K. Goeke, M.V. Polyakov, M. Vanderhaeghen, Prog. Part. in Nucl. Phys. **47** (2001) 401.

- [5] M. Diehl, Generalized Parton Distributions, DESY-thesis-2003-018, hep-ph/0307382.
- [6] A.V. Belitsky and A.V. Radyushkin, Phys. Rept. **418** (2005) 1.
- [7] M. Burkardt, Int. J. Mod. Phys. **A 18** (2003) 173.
- [8] "Exploring the 3D quark and gluon structure of the proton: Electron scattering with present and future facilities (JLab 12 GeV and EIC)" White Paper prepared for the discussion of the National Science Advisory Committee's Long Range Plan (2007).
- [9] J.W. Negele *et al*, Nucl. Phys. Proc. Suppl. 128 (2004) 170.
- [10] M. Goekeler *et al*, Nucl. Phys. Proc. Suppl. 140 (2005) 399.
- [11] P. Haegler *et al*, hep-lat/0705.4295 (2007), JLAB-THY-07-651, TUM-T39-07-09.
- [12] M. Strikman and C. Weiss, Phys. Rev. **D69** (2004) 054012.
- [13] J.C. Collins, L. Frankfurt and M. Strikman, Phys. Rev. **D56**, 2982 (1997).
- [14] H1 Collaboration, C. Adloff *et al.*, Phys. Lett. **B517** (2001) 47; A. Aktas *et al.*, Eur. Phys. J.C. **44** (2005) 1.
- [15] H1 Collaboration, A. Aktas *et al.*, Eur. Phys. J.C. **46** (2006) 585.
- [16] ZEUS Collaboration, S. Chekanov *et al.*, Phys. Lett. **B 573** (2003) 46.
- [17] ZEUS Collaboration, S. Chekanov *et al.*, Nucl. Phys. **B 695** (2004) 3.
- [18] CLAS Collaboration, S. Stepanyan *et al.*, Phys. Rev. Lett. **87** (2001) 182002.
- [19] CLAS Collaboration, S. Chen *et al.*, Phys. Rev. Lett. **97** (2006) 072002.
- [20] JLab Hall A Collaboration, C. Munoz Camacho *et al.*, Phys. Rev. Lett. **97** (2006) 262002.
- [21] JLab Hall A Collaboration, M. Mazouz *et al.*, accepted for publication in Phys. Rev. Lett.
- [22] HERMES Collaboration, A. Airapetian *et al.*, Phys. Rev. Lett. **87** (2001) 182001.
- [23] HERMES Collaboration, A. Airapetian *et al.*, Phys. Rev. **D 75** (2007) 011103.
- [24] HERMES Collaboration, F. Ellinghaus *et al.*, Nucl. Phys. **A 711** (2002) 171.
- [25] M. Diehl, T. Gousset, B. Pire, J. Ralston, Phys. Lett. **B 411** (1997) 193.
- [26] M. Diehl, contribution to the workshop "Future Physics @ COMPASS", 26-27 September 2002, CERN-2004-011.
- [27] A.V. Belitsky, D. Müller, A. Kirchner, Nucl. Phys. **B 629** (2002) 323.
- [28] M. Vanderhaeghen, P.A.M. Guichon, M. Guidal, Phys. Rev. Lett. **80** (1998) 5064; Phys. Rev. **D 60** (1999) 094017.

- [29] VGG code [28, 4]; implementation by L. Mossé.
- [30] M. Guidal, M.V. Polyakov, A.V. Radyushkin, M. Vanderhaeghen, Phys. Rev. **D 72** (2005) 054013
- [31] M. Diehl, Th. Feldmann, R. Jakob, P. Kroll, Eur. Phys. J. **C 39** (2005) 1
- [32] F. Ellinghaus, W.-D. Nowak, A.V. Vinnikov, and Z. Ye, Eur. Phys. J. **C46** (2006) 729, hep-ph/0506264.
- [33] J. Bisplinghoff *et al.*, Extraction of Transverse Target Spin Asymmetry for Exclusive ρ^0 Production from COMPASS 2002-2004, COMPASS-note 2007-9.
- [34] M. Diehl and S. Sapeta, Eur. Phys. J. **C41** (2005) 515, hep-ph/0503023;
M. Diehl, hep-ph/07041565v1.
- [35] G.V. Mescheryakov, A.P. Nagaytsev, I.A. Savin, Preliminary MC studies for measurements of GPD with COMPASS, COMPASS-note 2006-11;
O.P. Gavrishchuk *et al.*, Continuation of the MC studies of the ECAL0 design parameters for the measurements of GPD with COMPASS, COMPASS-note 2007-7.